

Apoptosis signal-regulating kinase I inhibition in *in vivo* and *in vitro* models of pulmonary hypertension

Kathryn S. Wilson¹, Hanna Buist¹, Kornelija Suveizdyte¹, John T. Liles², Grant R. Budas², Colin Hughes³, Margaret R. MacLean¹, Martin Johnson⁴, Alistair C. Church⁴, Andrew J. Peacock⁴ and David J. Welsh^{1,5}

¹Institute of Cardiovascular and Medical Sciences, University of Glasgow, Glasgow, UK; ²Gilead Sciences Inc., Foster City, CA, USA; ³Central Research Facility, University of Glasgow, Glasgow, UK; ⁴Scottish Pulmonary Vascular Unit, Golden Jubilee National Hospital, Clydebank, UK; ⁵Department of Biological and Biomedical Science, Glasgow Caledonian University, Glasgow, UK

Abstract

Pulmonary arterial hypertension, group 1 of the pulmonary hypertension disease family, involves pulmonary vascular remodelling, right ventricular dysfunction and cardiac failure. Oxidative stress, through activation of mitogen-activated protein kinases is implicated in these changes. Inhibition of apoptosis signal-regulating kinase I, an apical mitogen-activated protein kinase, prevented pulmonary arterial hypertension developing in rodent models. Here, we investigate apoptosis signal-regulating kinase I in pulmonary arterial hypertension by examining the impact that its inhibition has on the molecular and cellular signalling in established disease. Apoptosis signal-regulating kinase I inhibition was investigated in *in vivo* pulmonary arterial hypertension and *in vitro* pulmonary hypertension models. In the *in vivo* model, male Sprague Dawley rats received a single subcutaneous injection of Sugen SU5416 (20 mg/kg) prior to two weeks of hypobaric hypoxia (380 mmHg) followed by three weeks normoxia (Sugen/hypoxic), then animals were either maintained for three weeks on control chow or one containing apoptosis signal-regulating kinase I inhibitor (100 mg/kg/day). Cardiovascular measurements were carried out. In the *in vitro* model, primary cultures of rat pulmonary artery fibroblasts and rat pulmonary artery smooth muscle cells were maintained in hypoxia (5% O₂) and investigated for proliferation, migration and molecular signalling in the presence or absence of apoptosis signal-regulating kinase I inhibitor. Sugen/hypoxic animals displayed significant pulmonary arterial hypertension compared to normoxic controls at eight weeks. Apoptosis signal-regulating kinase I inhibitor decreased right ventricular systolic pressure to control levels and reduced muscularised vessels in lung tissue. Apoptosis signal-regulating kinase I inhibition was found to prevent hypoxia-induced proliferation, migration and cytokine release in rat pulmonary artery fibroblasts and also prevented rat pulmonary artery fibroblast-induced rat pulmonary artery smooth muscle cell migration and proliferation. Apoptosis signal-regulating kinase I inhibition reversed pulmonary arterial hypertension in the Sugen/hypoxic rat model. These effects may be a result of intrinsic changes in the signalling of adventitial fibroblast.

Keywords

pulmonary hypertension, mitogen-activated protein kinases, Sugen/hypoxic rat model

Date received: 2 October 2019; accepted: 6 April 2020

Pulmonary Circulation 2020; 10(2) 1–16

DOI: 10.1177/2045894020922810

Introduction

Pulmonary arterial hypertension (PAH), group 1 of the pulmonary hypertension (PH), is a multifactorial disease characterised by a sustained increased mean pulmonary arterial pressure (mPAP) ≥ 25 mmHg as a consequence of pulmonary vascular remodelling, infiltration of inflammatory cells,¹

Corresponding author:

David J. Welsh, Department of Biological and Biomedical Science, School of Health and Life Sciences, Glasgow Caledonian University, Glasgow G4 0BA, UK.
Email: David.Welsh@gcu.ac.uk



Creative Commons CC-BY: This article is distributed under the terms of the Creative Commons Attribution 4.0 License (<http://creativecommons.org/licenses/by/4.0/>) which permits any use, reproduction and distribution of the work without further permission provided the original work is attributed as specified on the SAGE and Open Access pages (<https://us.sagepub.com/en-us/nam/open-access-at-sage>).

© The Author(s) 2020.

Article reuse guidelines:
sagepub.com/journals-permissions
journals.sagepub.com/home/pul



thrombosis and neointima formation.^{2,3} These features result in increased pulmonary vascular resistance (PVR) and subsequent right ventricle (RV) overload, RV hypertrophy and eventual death. There is no cure for PAH, and available treatments act via vasodilation and anticoagulation but have limited therapeutic effect.^{4,5} In PAH, pulmonary vascular remodelling is a result of changes in cell hypertrophy and hyperplasia,⁶ apoptosis, migration and production of extracellular matrix (ECM).² The three main cellular sub-types of the vascular wall, endothelial cells (ECs), vascular smooth muscle cells and fibroblasts,⁷ are all implicated in PAH vessel remodelling; however, the adventitial fibroblast is one of the first cell types activated by vascular stressors.^{8–10}

Oxidative stress is markedly increased in patients with PAH and has been implicated in the changes to the pulmonary vasculature and RV. These changes are thought to be as a result of an imbalance of anti-oxidative and pro-oxidative enzymes increasing levels of reactive oxygen species (ROS) which can compromise vascular cell function.^{11–14} In animal PAH models, elevated levels of ROS have been observed and antioxidant agents have been shown to have beneficial therapeutic effects.^{15–17} The adventitial fibroblast, in response to environmental stresses, produces ROS leading to phenotypic changes within the cell and are thought to contribute to the thickening and fibrosis of the adventitia observed in vasculopathies such as PAH.¹⁸

ROS are involved in the regulation of cell signalling pathways¹⁸ such as mitogen-activated protein kinase (MAPK) pathways.^{19,20} MAPKs are associated with a variety of cellular effects including proliferation, survival, death and transformation.²¹ *In vitro* studies demonstrate that acute hypoxia increases proliferation in pulmonary artery fibroblasts (PAFs) in a p38 MAPK-dependent response; furthermore, inhibition of p38 MAPK in rodent PAH models prevents the disease phenotype.²² The role of ROS in MAPK activity was demonstrated in the blockade of MAPK activation in lipopolysaccharide (LPS)-stimulated cells by the introduction of antioxidants^{23,24}; furthermore, the addition of oxidative stress mimetics induces MAPK signalling.²⁵

Apoptosis signal-regulating kinase 1 (ASK1) is a constitutively expressed MAPK, which selectively activates the Jun N-terminal kinase (JNK) and p38 MAPK pathways in response to various stressors, including oxidative stress. ASK1 is ordinarily repressed by thiol-containing thioredoxins; however, in instances of elevated oxidative stress, thioredoxin undergoes oxidation and dissociation from ASK1 leading to ASK1 activation and phosphorylation of downstream MAPKs.^{26,27} A number of studies using ASK1-deficient mice highlight the importance of ASK1 in many stress-related diseases.²⁸ The possibility that small compound inhibitors of ASK1 activity could ameliorate disease development and/or progression has been demonstrated in a study using an orally administered ASK1 inhibitor in experimental PAH.²⁹ ASK1 inhibition in this study reduced

maladaptive remodelling of the RV and pulmonary vasculature, with corresponding increases in RV function and vasoreactivity in PAH rodent models.^{29,30} A recent Phase 2 clinical trial (ARROW trial NCT02234141), testing a first-in-class ASK1 inhibitor in PAH patients, however, did not demonstrate a significant change in PVR (primary endpoint), although no adverse side-effects were noted.³¹ It is clear from the discrepancy between the pre-clinical and clinical data that further investigation is required into the underlying cellular mechanisms by which ASK1 inhibition results in reduced pulmonary vascular remodelling in rodent models. In the present study, we confirm the findings previously documented and further investigate the cellular changes which occur.

Methods

An expanded methodology section can be found in online Supplement.

In vivo study

All experimental procedures were carried out in accordance with the United Kingdom Animal Procedures Act (1986), conform to the guidelines from directive 2010/63/EU of the European Parliament on the protection of animals used for scientific purposes and with the 'Guide for the Care and Use of Laboratory Animals' published by the US National Institutes of Health (NIH publication No. 85-23, revised 1996). Local ethical approval was also granted.

See online Supplement for housing details, the Sugeng/hypoxic (SuHx) rat model, drug treatment and GS-444217 pharmacokinetic data. Briefly, male Sprague Dawley rats (three weeks old) were divided into four groups. Group 1: SuHx + V – a single subcutaneous dose of Sugeng-5416 (Sigma-Aldrich, Irvine, UK) suspended in vehicle (20 mg/kg), then housed in a hypobaric chamber (atmospheric pressure 550 mbar) for two weeks (weeks 0 → 2) then housed at normal room pressure (1013 mbar) for three weeks (weeks 2 → 5) and given a control chow throughout (weeks 0 → 8). Group 2: SuHx + GS – as for Group 1, however, animals received GS-444217 chow (weeks 5 → 8). Group 3: Norm + V – a single subcutaneous dose of vehicle, maintained at normal room pressure for five weeks (weeks 0 → 5) and given a control chow throughout (weeks 0 → 8). Group 4: Norm + GS – as for Group 3, however, animals received GS-444217 chow (weeks 5 → 8) (summarised in online Supplemental Fig. 1). Animals were weighed at the end of the study.

Haemodynamic measurements. Haemodynamic measurements were obtained in a cohort of animals at five weeks and another cohort of animals at eight weeks. Animals were anaesthetically induced by inhalation in 3% (v/v) isoflurane and then maintained at 1.5–2% (v/v) isoflurane

supplemented with a constant flow of 5% (v/v) oxygen. Haemodynamic measurements were taken using an ultra-miniature polyimide nylon catheter (SPR-869NR, Millar, Houston, TX, USA) as per the manufacturer's instructions with the PowerLab 35 Series data acquisition system and LabChart Pro (AD instruments, Oxford, UK) using the pressure volume (PV) Loop analysis module. The catheter was inserted into the jugular vein and guided into the RV of the heart to measure right ventricular systolic pressure (RVSP). After RVSP was determined, the carotid artery was isolated and the same catheter was inserted to determine systolic arterial pressure (SAP). The PV loop system also generated heart rate and cardiac output (CO) data. On removal of the catheter, blood was collected immediately to obtain both serum and plasma fractions, these were used for further analysis by enzyme-linked immunosorbent assay (ELISA). Subsequently, animals were euthanized by terminal anaesthesia through inhalation overdose 5% (v/v) isoflurane with a constant flow of 5% (v/v) oxygen until cessation of breathing as approved by the local ethics committee.

Right ventricular hypertrophy and tissue harvest. Immediately following hemodynamic assessment, animals were culled and tissues were harvested for further analysis. The heart and lungs were flushed with ice-cold phosphate buffered saline (PBS) at a low pressure using a blunt needle to clear peripheral blood cells. The right lung was tied off with suture and excised for molecular analysis. In a cohort of animals from each group, the hearts were isolated, atria removed and separated to give RV and left ventricle (LV). These were weighed separately and right ventricular hypertrophy (RVH) was assessed by the Fulton Index ((dry weight of the RV)/(dry weight of the LV + septum)). In the remaining animals from each group, the heart was excised whole and fixed with 10% (v/v) neutral buffered formalin (NBF) for 48 h under mild agitation before paraffin processing and embedding for immunohistological analysis. Large pulmonary arteries (PAs) were dissected for rat pulmonary artery fibroblasts (RPAFs) isolation and the left lung was inflated and fixed with 10% (v/v) NBF as for hearts.

Immunohistology. 5 µm lung and heart sections were cut, from paraffin blocks and mounted on Superfrost® microscope slides (Sigma-Aldrich, Irvine, UK).

Vascular thickening was determined by smooth muscle actin antibody (ab5694, Abcam, Cambridge, UK) staining, thickening was characterised by an increase in the vessel wall diameter of more than 50% of the arterial wall or complete occlusion. The number of remodelled vessels over the total number of vessels present in a lung section was determined. Sections were analysed in a blinded manner.

Heart sections were stained using a common regressive Haemotoxylin and Eosin (H&E) staining methodology to determine gross morphology and cardiomyocyte cross-sectional area. High-power images of five areas randomly

distributed across ventricles were analysed by ImageJ software. Mean cardiomyocyte size was determined by measuring the cross sectional area of minimally 20 transversally cut cardiomyocytes at the level of the nucleus.

Picro-sirius red staining was used for analysis of cardiac fibrosis using a Picro-sirius red staining kit (Abcam, Cambridge, UK) as per manufacturer's instructions. High-power images were acquired of five random areas per ventricle. Using ImageJ IHC tool, the percentage tissue area positive for collagen (pink) was determined.

In vitro study

Primary cell culture and exposure to hypoxia. RPAFs and rat pulmonary artery smooth muscle cells (RPASMCs) were produced by primary cell culture of PAs dissected free from the lung and heart of adult male Sprague Dawley rats (either wild-type animals or those which were part of the *in vivo* study). Tissue was manually manipulated to culture either RPAFs or RPASMCs using an adaption of the explant technique by Freshney³² and summarised in online Supplement. Cells were maintained under standard culture conditions³³ in the presence of serum or were exposed to hypoxia as an *in vitro* model of PH by incubation in a variable O₂ humidified temperature-controlled chamber (5% CO₂ in air at 37°C) with a PO₂ maintained at 35 mmHg.³³ All cellular experiments are carried out as biological replicates.

RPASMC culture in RPAF conditioned media. RPAF were cultured until 80% confluent and quiesced in serum-free Dulbecco's Modified Eagle's Medium (DMEM) for 24 h before being cultured in hypoxic or normoxic culture conditions (as above) for 24 h whereby culture media (CM) was collected. RPASMC were cultured until 50–60% confluence then quiesced for 24 h in serum free media. Media was aspirated from cells and RPAF CM was added to each well for further analysis in the presence or absence of GS-444217.

RPAF and RPASMC co-culture. RPAFs were seeded in 12-well inserts (ThinCert™, Greiner Bio-One, Stonehouse, UK). RPASMCs were cultured in 12-well plates and at 50–60% confluence, then quiesced for 24 h. RPAF inserts were transferred into the RPASMC-containing wells, cells were cultured with and without GS-444217 in either normoxic or hypoxic conditions, RPAF inserts were removed prior to analysis.

Cell proliferation. RPAF were grown in 24-well culture plates in normal culture conditions (as above) until 60% confluent. Cells were quiesced in serum-free DMEM for 24 h then cultured under normoxic or hypoxic conditions in the presence or absence of varying concentrations of serum for 24 h with or without the ASK1 inhibitor. Two methods of cell counting were used, [³H] thymidine incorporation and automated cell counter, and comparable results were obtained (protocols are summarised in online Supplement).

Cell migration. The ‘scratch’ assay was used to determine cell migration over a 24-h period following cellular manipulation (further detail in online Supplement).

Preparation of GS-444217. GS-444217, a potent and selective small-molecule inhibitor of ASK1, was synthesised by Gilead Sciences Inc. (Foster City, USA) and was reconstituted in low percentage (<0.1%) dimethyl sulphoxide and suspended in DMEM. The ASK1 inhibitor was used throughout at a concentration of 1 μ M.

Protein analysis

Protein abundance in tissue homogenate and RPAFs was determined by immunoblotting, densitometry and normalised to total p38 MAPK as housekeeper/loading control as described in online Supplement.

Enzyme-linked immunosorbent assays

ELISAs were carried out to quantify the levels of key cytokines. These included rat soluble intracellular adhesion molecule 1 (sICAM-1), rat tissue inhibitor of metalloproteinases 1 (TIMP-1) (both from R&D Systems) and Endothelin-1 (ET-1) (Enzo Life Sciences, Exeter, UK), all ELISAs were carried out as per manufacturer’s instructions.

Statistical analysis

In vivo experiments are $n=4-6$ per experimental group and *in vitro* experiments were $n=3-6$ unless otherwise stated. Data are expressed as means \pm standard error of the mean. Treatments were compared by one-way or two-way repeated measures analysis of variance with appropriate post hoc tests highlighted in relevant text. A p value <0.05 was considered statistically significant.

Results

ASK1 inhibition reverses cardiopulmonary parameters associated with PH in the SuHx rat model

At eight weeks, RVSP was raised in the SuHx + V group compared to Norm + GS and SuHx + GS (46.68 ± 6.51 mmHg vs 29.59 ± 1.26 and 25.18 ± 2.97 mmHg respectively) (Fig. 1a)). While body weight was found to be decreased in SuHx groups, neither SuHx nor ASK1 inhibitor altered any other cardiac parameters measured (SAP heart rate and CO) (Fig 1b–e). The SuHx + V group displayed significantly greater RV hypertrophy compared to the Norm + V; the addition of GS-444217 did not significantly reduce RV hypertrophy (Fig. 1f). Morphologically, SuHx + V hearts appeared to have considerable RV free wall thickening which was not observed in any other groups (as highlighted on histological images; Figs 1g–j). Cardiomyocyte area, as determined by mean cell area

(Pixels) of high magnification images of H&E-stained heart sections (Fig. 1k), was found to be significantly increased in the SuHx + V group compared to all other groups with SuHx + GS comparable to both Norm + V and Norm + GS (Fig. 1l). RV fibrosis as determined by Picro-sirius red stain (Fig. 1m) highlighted more fibrosis (Picro-sirius positive area) in the SuHx + V group compared to all other groups (Fig. 1n).

Alpha smooth muscle actin staining was carried out on lung sections to determine pulmonary vascular remodelling (Fig. 2a), this stain highlighted a greater number of remodelled vessels in the SuHx + V group compared to both Norm groups, the addition of GS-444217 in the SuHx + GS group prevented this rise (Fig. 2b).

Phospho-p38 MAPK (pp38 MAPK) protein abundance in whole tissue homogenate was determined by Western blot analysis. An increase in pp38 MAPK relative abundance was observed in lung homogenate from SuHx + V animals compared to Norm + V, Norm + GS and SuHx + GS (Fig. 2c). In the right ventricular tissue homogenates, there was a rise in the abundance of pp38 MAPK levels in SuHx + V animals compared to both normoxic groups, while a reduction was noted in SuHx + GS, this was not found to be statistically significant (Fig. 2d). No detectable difference in pp38 MAPK was determined in LV tissue homogenates (Fig. 2e). Phospho-ASK1 (pASK1) was also investigated by Western blot and demonstrated a significant increase in abundance in the lung of SuHx + V compared to Norm + GS and SuHx + GS lung tissue (Fig. 2f) similar observations were noted in LV and RV – data not shown).

Plasma from all groups was analysed for potential biomarkers. Circulating ET-1 was significantly raised in SuHx + V animals compared to SuHx + GS (Fig. 2g). Similarly, in SuHx + V animals, circulating TIMP-1 was significantly raised compared to all other groups, SuHx + GS was comparable to both normoxic groups (Fig. 2h). Circulating levels of B-type natriuretic peptide (BNP) were also significantly raised in SuHx + V animals compared to Norm + V controls. In the presence of GS-444217, BNP levels were comparable to controls (Norm + V and Norm + GS) with a trend towards significant reduction compared to SuHx + V ($p=0.055$ (Fig. 2i)).

ASK1 inhibitor prevents remodelling features in RPAF cells cultured from the SuHx rat model

RPAFs were cultured from isolated PAs from either Norm + V, SuHx + V or SuHx + GS animals and were then investigated further. Using a scratch assay, the migratory capacity of these RPAFs cultured with differing concentrations of serum was investigated. SuHx + V and SuHx + GS were found to have significantly greater migration to Norm + V cells at all three serum concentrations. SuHx + GS cells were also found to migrate significantly less than SuHx + V cells (Fig. 3a) at all serum levels.

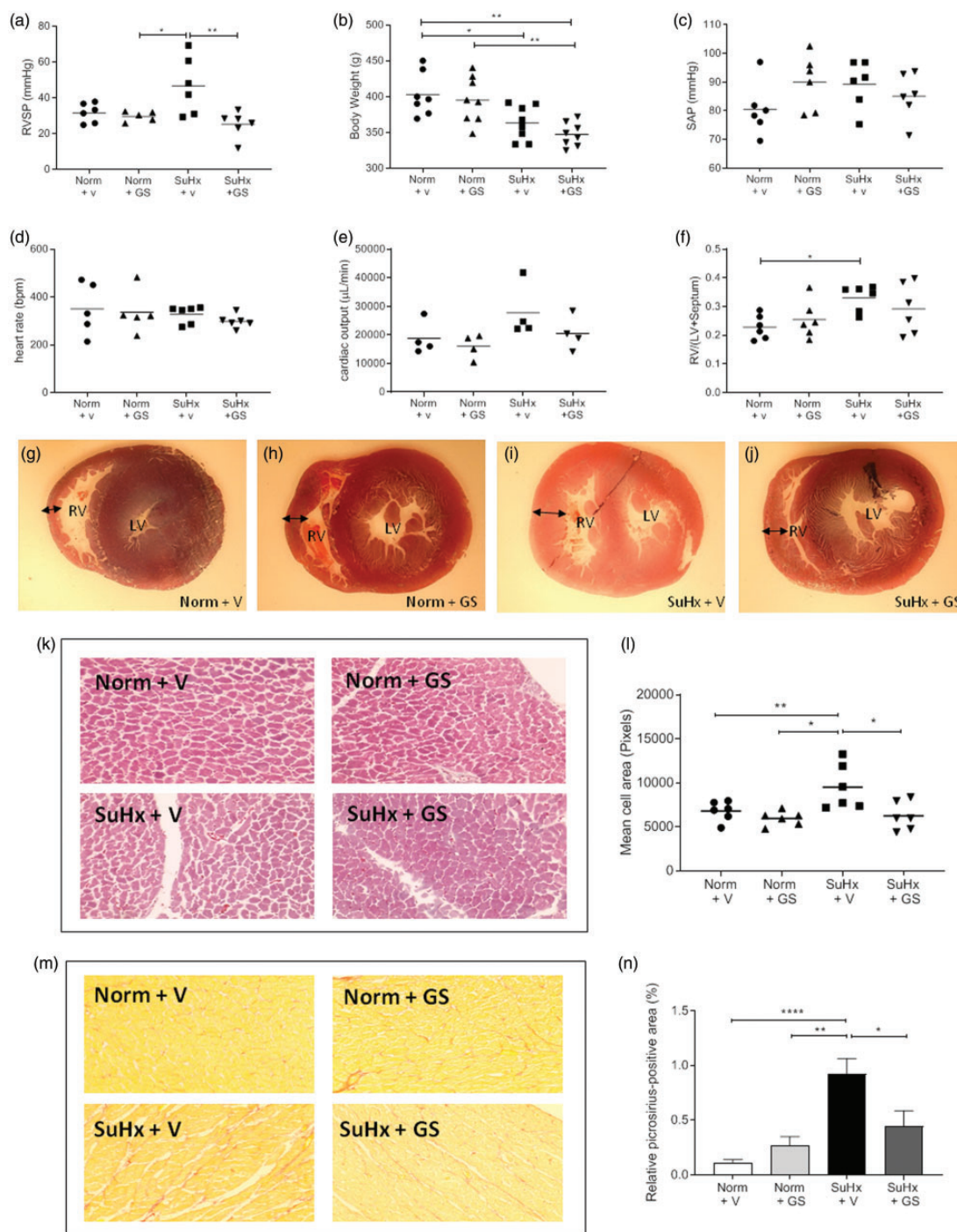


Fig. 1. Sugen/hypoxic rat haemodynamic and cardiac characteristics after ASK1 inhibition. The impact of ASK1 inhibitor GS-44217 in reversing established pulmonary hypertension (PH) was investigated in the Sugen/hypoxic (SuHx) rat model. Four groups of animals were investigated; SuHx animals treated with vehicle (SuHx + V) or the ASK1 inhibitor GS-44217 (SuHx + GS) for three weeks post disease establishment (at five weeks) or age-matched normoxic controls treated with vehicle (Norm + V) or drug (Norm + GS). Parameters investigated were (a) right ventricular systolic pressure (RVSP), (b) body weight, (c) systemic arterial pressure (SAP), (d) heart rate, (e) cardiac output, (f) right ventricular hypertrophy, (g–j) representative images of transverse heart histological sections stained with haematoxylin (double arrows highlight RV free wall thickening), (k) cardiomyocyte cross-sectional area determined from high-powered magnification images of haematoxylin-stained transverse whole heart sections and (l) quantification by post hoc ImageJ analysis, (m) collagen content determined in heart sections stained with Picro-sirius red stain and (n) quantification by post hoc ImageJ analysis. Data are (a, c, d and f) $n = 6$ animals per group, (b) $n = 7/8$ animals per group, (e) $n = 4$ animals per group, displayed as individual data points and mean; (l and n) $n = 6$ animals (mean of four sections per heart) displayed as individual data points and mean (l) or mean \pm SEM (n). Statistical analysis is by two-way ANOVA with Turkey's post hoc analysis * $p \leq 0.05$ and ** $p \leq 0.01$, *** $p \leq 0.001$.

RV: right ventricle; LV: left ventricle.

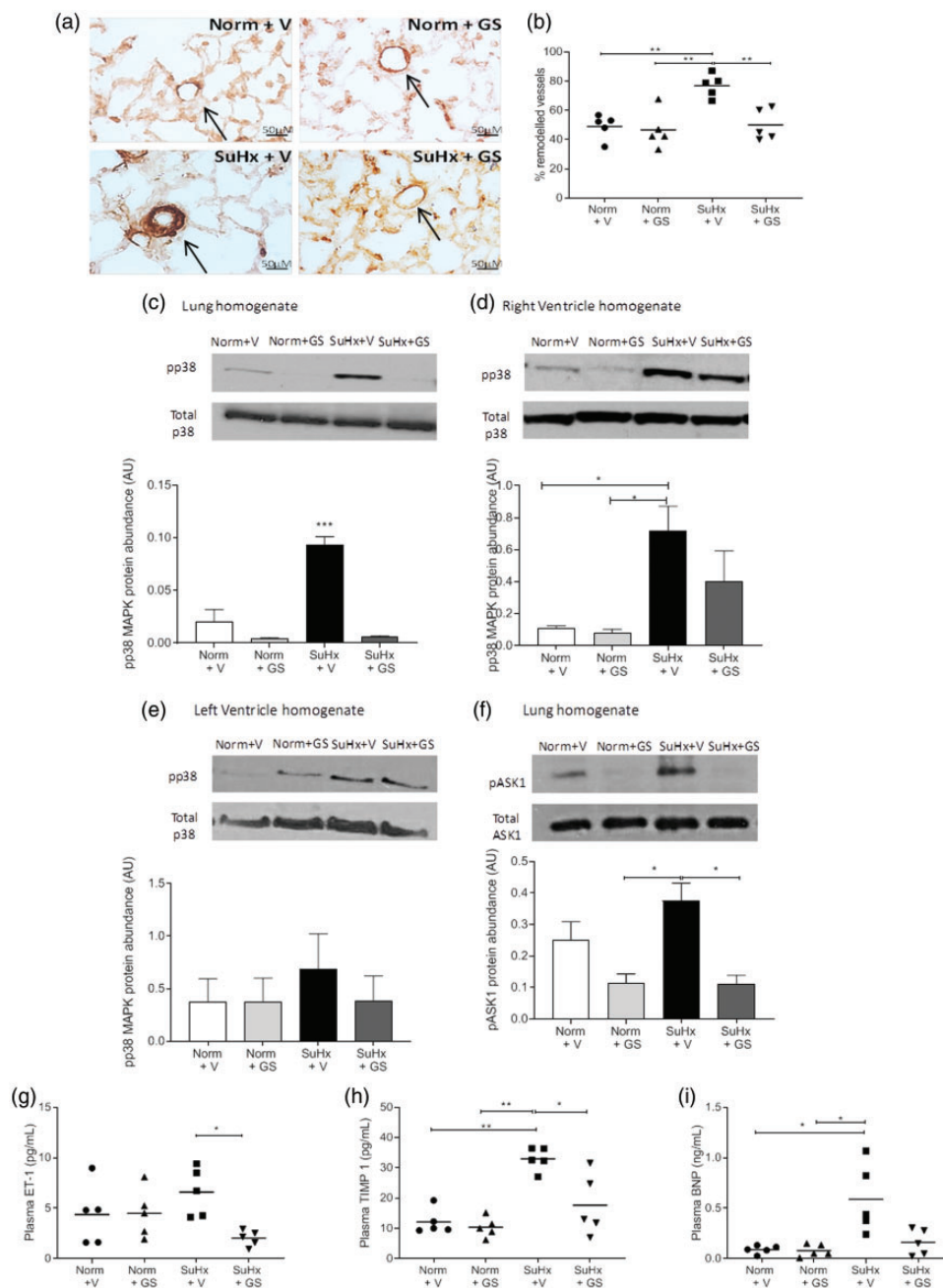


Fig. 2. Sugen/hypoxic rat cardiopulmonary cardiac characteristics after ASK1 inhibition. The impact of ASK1 inhibitor GS-44217 in reversing established pulmonary hypertension (PH) was investigated in the Sugen/hypoxic (SuHx) rat model. Four groups of animals were investigated; SuHx animals treated with vehicle (SuHx + V) or ASK1 inhibitor GS-44217 (SuHx + GS) for three weeks post disease establishment (at five weeks) or age-matched normoxic controls treated with vehicle (Norm + V) or drug (Norm + GS). (a) Pulmonary vascular remodelling was investigated through analysis of high-power magnification images of lung α smooth muscle actin (α -SMA) immunohistochemistry, arrows show pulmonary vessels of interest and (b) and pulmonary vascular remodelling quantification. (c–f) Protein abundance determined and quantified by Western blot analysis in tissue homogenate for phospho p38 MAPK (pp38 MAPK) in (c) lung, (d) right ventricle (RV), (e) left ventricle (LV) and (f) phospho ASK1 (pASK1) in lung. All protein abundance is normalised to total p38 MAPK (tp38 MAPK) and is presented as relative abundance (AU). Data are $n = 4$ biological replicates per group and are displayed as mean \pm SEM analysed by one-way ANOVA with Turkey's post hoc analysis. * $p \leq 0.05$. Plasma analysis was also carried out to quantify the levels of (g) endothelin-1 (ET-1), (h) tissue inhibitor of metalloproteinases (TIMP1) and (i) B-type natriuretic peptide (BNP). Quantification data is $n = 5$ per group for all plasma analyses and displayed as individual data points with mean. Statistical analysis is by one-way ANOVA with Turkey's post hoc analysis * $p \leq 0.05$ and ** $p \leq 0.01$. MAPK: mitogen-activated protein kinase; ASK1: apoptosis signal-regulating kinase I.

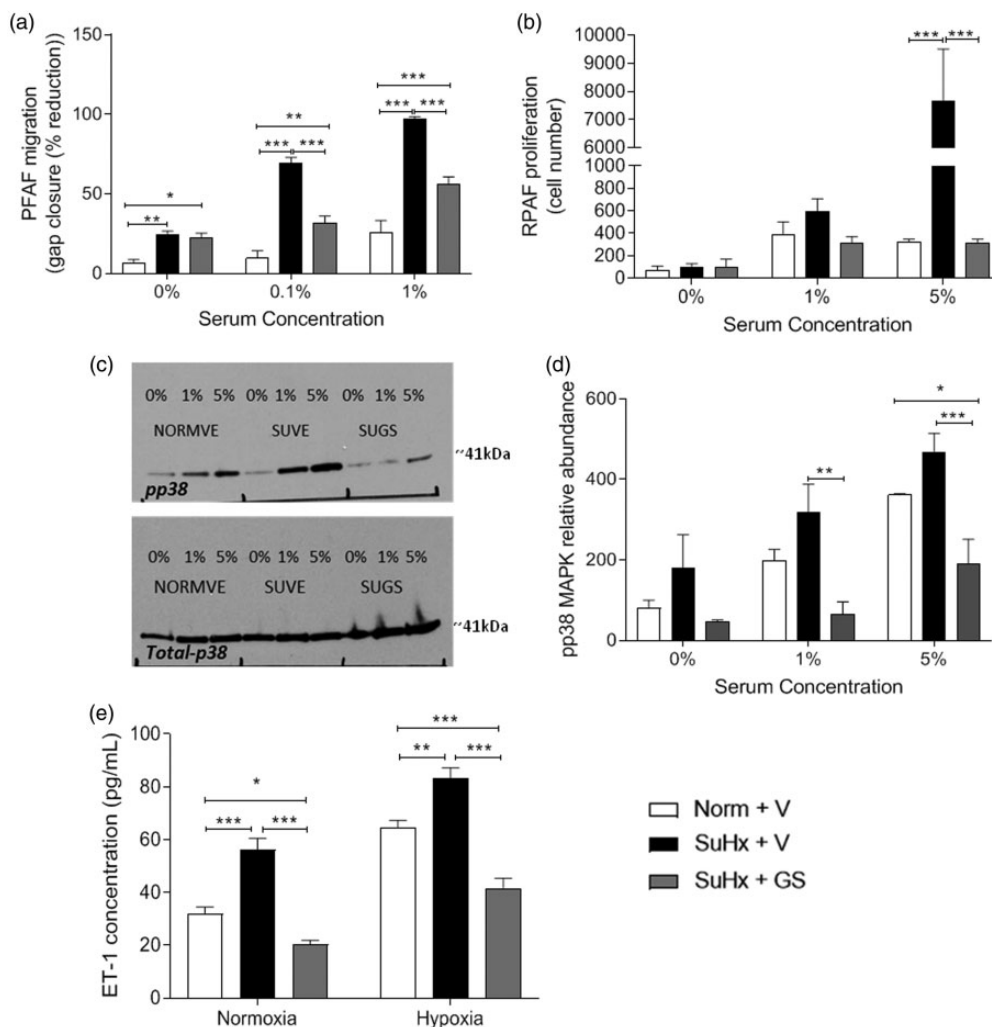


Fig. 3. Phenotypic characteristics of study animal cells. Rat pulmonary artery fibroblasts (RPAFs) were cultured from SuHx animals treated with vehicle (SuHx + V) or GS-444217 (SuHx + GS) or normoxic controls. (a) Cellular migration was investigated in each group following incubation with varying but sub-proliferative concentrations of serum and was determined using scratch assay then quantified as percent gap closure. (b) Proliferation was investigated in each group following incubation with varying but pro-proliferative concentrations of serum and was determined using an automated cell counter and displayed as cell number. (c and d) Phospho p38 mitogen-activated protein kinase (pp38 MAPK) protein abundance was determined in cells with varying concentrations of serum by Western blot and graphically displayed relative to total p38 MAPK (tp38 MAPK) levels. (e) Cell culture conditioned media analysis was also carried out to quantify the levels of endothelin-1 (ET-1) from RPAFs cultured from experimental animals maintained in normoxic or hypoxic culture conditions. Data are $n = 4$ and represented as mean \pm SEM, and are analysed by two-way ANOVA and Tukey's post hoc analysis. $*p \leq 0.05$, $**p \leq 0.01$ and $***p \leq 0.001$.

Cell proliferation was investigated following the addition of serum. No significant difference in cell proliferation was noted between cells at 0 and 1% serum; however, at 5% serum, a significant rise in proliferation was noted in SuHx + V cells compared to both Norm + V and SuHx + GS cells (Fig. 3b).

RPAF cells were further investigated at increasing serum concentrations to determine pp38 MAPK abundance by Western blot (Fig. 3c). A rise in pp38 MAPK was observed in each group with increasing serum levels; when comparing the groups at a given serum concentration, the levels were significantly lower for SuHx + GS cells compared to SuHx + V (1% serum 65.47 ± 31.01 vs 319.58 ± 68.34

abundance AU; 5% 191.43 ± 59.83 vs 469.07 ± 45.41 AU, Fig. 3d).

Conditioned media from cells from all three groups maintained either in normoxia or hypoxia for 24 h was investigated by ET-1 ELISA. It was observed that in normoxic conditions, cells from the SuHx + V animals produced significantly more ET-1 than cells from Norm + V animals (56.12 ± 9.94 vs 33.32 ± 5.09 pg/mL) and that cells from SuHx + GS animals had significantly lower levels of ET-1 than Norm + V. Similarly, cells which were incubated in hypoxic conditions demonstrated the same pattern of ET-1 levels; however, values were raised compared to normoxia (Fig. 3e).

*ASK1 inhibitor alters signalling pathways of wild-type RPAFs in an *in vitro* model of PH*

A significant increase in hypoxia-inducible factor (HIF)-1 α , pASK1, extracellular signal-regulated kinase 1/2 (ERK1/2) and pp38 MAPK protein abundance was observed in hypoxic cells both in the presence or the absence of 1% serum when compared to cells grown in normoxia. These increases in abundance were not observed in cells which were pre-incubated with the ASK1 inhibitor GS-444217. The relative abundance of phospho-mitogen activated-kinase kinase 3/6 (pMKK3/6) and pJNK were also investigated; however, there was no change in levels detected in cells which were cultured in hypoxic conditions with or without serum (Fig. 4a–g). Cytokine levels were studied in RPAF CM using ELISAs. sICAM-1 levels were increased in hypoxic cells compared to normoxic cells and with the addition of ASK1 inhibitor; levels were comparable to controls (Fig. 4h). Hypoxic conditions had no impact on the detectable levels of TIMP-1 in CM; the addition of serum, however, did significantly increase levels which were prevented by the addition of GS-444217 (Fig. 4i). RPAFs cultured in hypoxia displayed increased levels of ET-1, however, in the presence of GS-444217. ET-1 levels in the hypoxic cells were reduced to levels comparable to normoxic controls (Fig. 4j).

*ASK1 inhibitor prevents remodelling characteristics of wild-type RPAFs in an *in vitro* model of PH*

In an *in vitro* model of PH-acute hypoxia, wild-type RPAF displayed increased proliferation compared to normoxia which GS-444217 prevented, with a four-fold reduction in proliferation to levels reaching that of normoxic cells (Fig. 5a). GS-444217 had no effect on wild-type RPASMC proliferation in either normoxic or hypoxic conditions (Fig. 5b). RPASMCs co-cultured with RPAF and maintained in normoxia (Norm CC) displayed no detectable difference in proliferation; however, a significant increase was noted when co-cultured with RPAF in hypoxic conditions. GS-444217 reduced this proliferation by ~50%. There was no change in the proliferative response of RPASMCs cultured in normoxic RPAF CM (Norm CM); however, increased proliferation was noted in hypoxic RPAF CM (Hyp CM). GS-444217 had no effect on CM-mediated RPASMC proliferation (Fig. 5d).

GS-444217 did not affect RPAF migration under normoxic conditions (Fig. 5e); however, in hypoxic cells, a significant increase in migration was observed, the addition of GS-444217 prevented migration. In RPASMC, incubation of GS-444217 had no effect on migration in normoxic or hypoxic cells (Fig. 5f). RPASMC with Hyp CC displayed an enhanced migratory response, compared to RPASMC cultured alone, which was prevented by GS-444217 (Fig. 5g). RPASMCs cultured in Hyp CM displayed enhanced migration compared to Norm CM. The addition of GS-444217 did not prevent scratch closure (Fig. 5h).

To determine whether ET-1 mediated RPASMC phenotypic changes, cells were incubated with increasing concentrations of ET-1 and were then assessed for proliferative and migratory capacity. First, it was determined that ET-1 was capable of increasing both proliferation and migration of RPASMC at 0.5 and 1 μ M when compared to control cells (Fig. 6a and b). To determine whether ET-1 released from RPAFs was responsible for RPASMC phenotype changes, RPASMC cells were incubated in RPAF conditioned media from normoxic or hypoxic culture with or without the addition of the endothelin receptor antagonist, Ambrisentan. As previously shown, only the addition of hypoxic CM resulted in increased RPASMC proliferation; however, the addition of Ambrisentan prevented the increase in proliferation (Fig. 6c). Migration was also investigated using scratch assay (Fig. 6d), as before hypoxic condition media was the only media which resulted in almost complete gap closure, the addition of Ambrisentan prevented this migratory response (Fig. 6e).

Discussion

PAH is a debilitating disease with poor survival rates and, whilst life-prolonging, current PAH treatments do little to address the underlying cellular and molecular changes in the heart or the vasculature. Our group has previously highlighted the importance of MAPK signalling, particularly through p38 MAPK, in experimental models of PAH²²; however, the apical MAP3K responsible for these changes has, until recently, been poorly characterised in this disease. The recent study by Budas et al. was the first to describe a pathological role of the MAP3K ASK1 in maladaptive remodelling of the pulmonary vasculature and RV supporting rationale for ASK1 inhibition as a novel therapeutic strategy for PAH.²⁹ Whilst Budas and colleagues highlight a role of ASK1 in disease pathogenesis and discussed possible cellular mechanisms involved in cardiac fibrogenesis, less is known about the role ASK1 plays in pulmonary vascular remodelling. The results of the presented study not only support the preclinical findings of Budas et al. but also address the underlying cellular mechanisms.

The present study investigates ASK1 inhibition in the SuHx *in vivo* model where PAH occurs as a result of vascular endothelial growth factor (VEGF) receptor blockade concurrently with chronic hypoxia resulting in precapillary arterial occlusion.³⁴ Where our study differs from the previous study²⁹ is that we use the now more commonly used model of a single dose of 20 mg/kg SU5416 at the commencement of hypoxic phase followed by three weeks normoxia prior to treatment compared to 200 mg/kg and three weeks hypoxia only. While both models have been used extensively in PAH study, lower dose SU5416 is known to be sufficient for PAH-like features which worsen in normoxia, developing into complex vascular lesions.³⁵ We confirm that disease was established after five weeks (online Supplemental Fig. 2) and as such we believe this a more

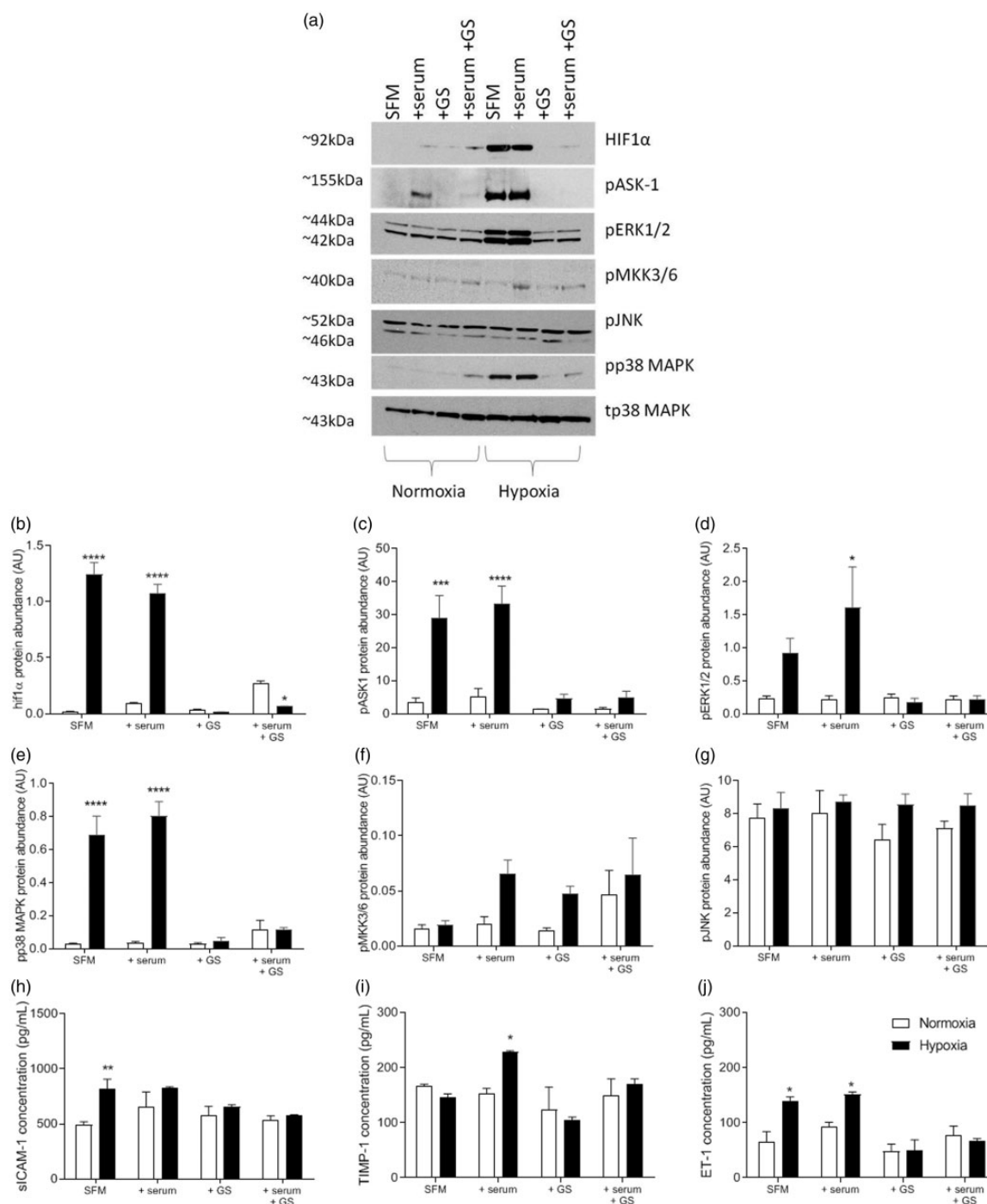


Fig. 4. ASK1 inhibition prevents hypoxia-induced increases in protein abundance in rat pulmonary artery fibroblasts (RPAFs) derived from wild-type animals. RPAF were exposed to either normoxic or hypoxic culture conditions for 24 h in the presence or absence of 1% serum (+serum), with or without the ASK1 inhibitor GS-444217 (+GS), protein abundance was determined in the resulting cell lysate by Western blot analysis. (a) Typical Western blots of the hypoxia-induced transcription factor HIF-1 α , phosphorylated (p) ASK1, MKK3/6, MKK4, JNK and p38 MAPK. Total (t) p38 MAPK is used here as a house-keeping protein and loading control for densitometry of Western blots to determine protein relative abundance. Protein abundance was graphically represented as bar chart as mean \pm SEM for ease of interpretation. All stats are vs normoxic controls analysed by one-way ANOVA and Bonferroni's multiple comparison test. * $p \leq 0.05$ and ** $p \leq 0.01$. Cell culture conditioned media analysis was also carried out to quantify the levels of (h) soluble intracellular adhesion molecule 1 (sICAM-1), (i) tissue inhibitor of metalloproteinases (TIMP1) and (j) endothelin-1 (ET-1). Quantification data are $n = 5$ per group for all plasma analyses and displayed as individual data points with error bars representing mean \pm SEM. Statistical analysis is by one-way ANOVA with Turkey's post hoc analysis. * $p \leq 0.05$ and ** $p \leq 0.01$. SFM: serum free media; HIF-1 α : hypoxia-inducible factor-1 α ; pASK1: phospho apoptosis signal-regulating kinase 1; pp 38 MAPK: phospho p38 mitogen-activated protein kinase.

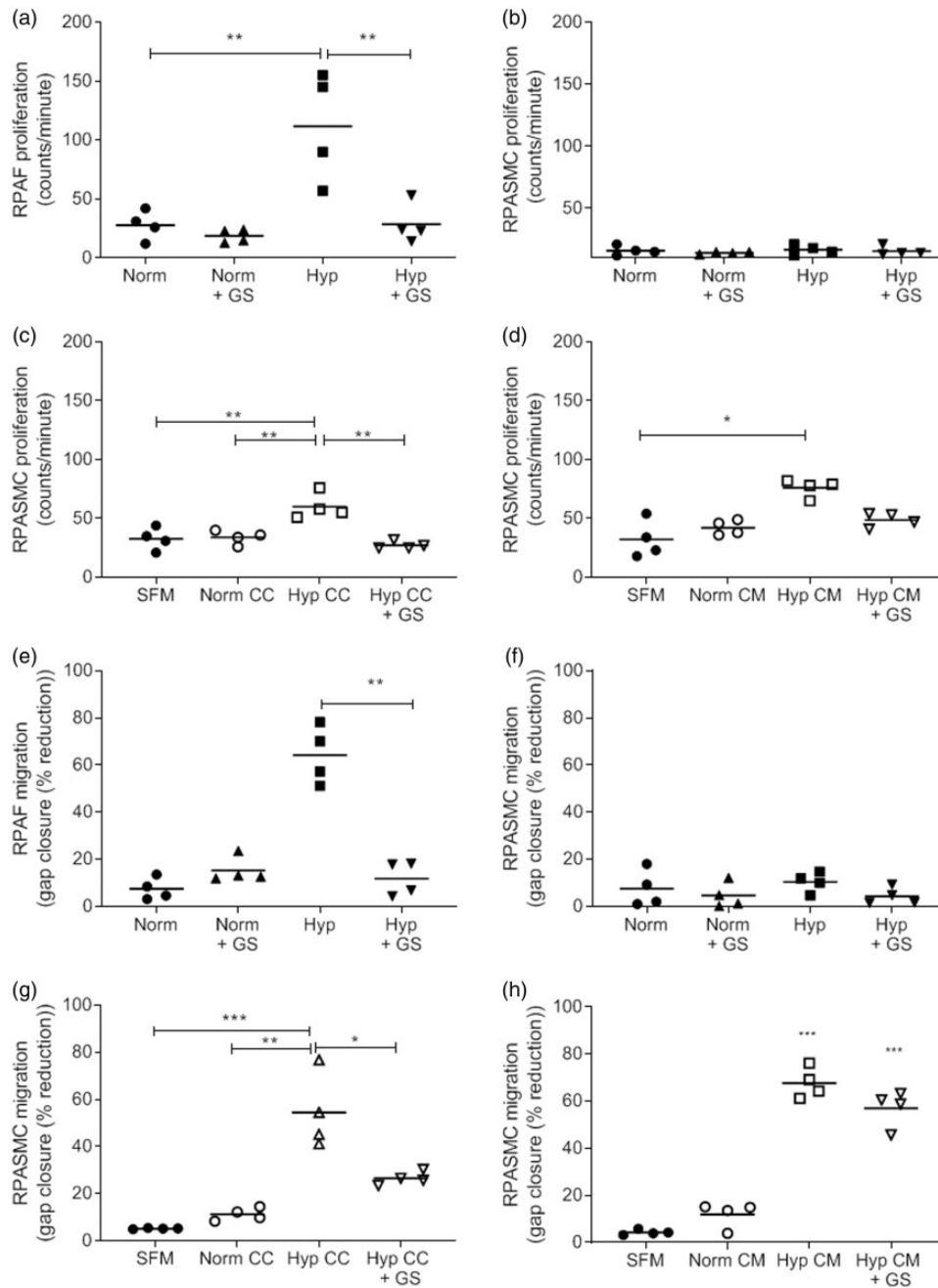


Fig. 5. Effects of ASK1 inhibition on hypoxia-induced rat pulmonary artery fibroblast and smooth muscle cell proliferation and migration. Proliferation was determined by [³H] thymidine incorporation assay in rat pulmonary artery fibroblasts (RPAFs) and rat pulmonary artery smooth muscle cells (RPASMCs). (a and b) Proliferation of RPAFs and RPASMCs (counts/min) was determined in cells exposed to either normoxic or hypoxic culture conditions with or without the ASK1 inhibitor GS-444217 for 24 h. (c) RPASMC proliferation was determined in cells grown in co-culture with RPAFs, groups investigated are RPASMC cultured in serum free media (SFM), those co-cultured with RPAFs in normoxic conditions (Norm CC), those cultured with RPAFs in hypoxic conditions (Hyp CC) and those cultured with RPAFs in hypoxic conditions in the presence of GS-444217 (Hyp CC + GS). (d) RPASMC proliferation determined in cells grown in the presence or absence of conditioned culture media (CM-media used previously to culture RPAF cells in various culture conditions). Groups investigated are RPASMC cultured in serum free media (SFM), those cultured with CM from normoxic RPAFs (Norm CM), those cultured with CM from hypoxic (Hyp CM) RPAFs and those cultured in CM from hypoxic RPAFs in the presence of GS-444217 (Hyp CM + GS). Migration was determined by scratch closure assay in RPAFs and RPASMCs. (e and f) Migration of RPAFs and RPASMCs (% reduction) was determined in cells exposed to either normoxic or hypoxic culture conditions with or without the ASK1 inhibitor GS-444217 for 24 h. (g) RPASMC migration was determined in cells grown in co-culture with RPAFs, groups investigated are RPASMC cultured in SFM, Norm CC, Hyp CC and Hyp CC + GS. (h) RPASMC migration was determined in cells grown in the presence or absence of conditioned CM, groups investigated are RPASMC cultured SFM, Norm CM, Hyp CM and Hyp CM + GS. Proliferation data are $n=4$ and migration data are $n=3$, all are displayed as individual data points with mean. Statistical analysis is by one-way ANOVA and Tukey or Bonferroni multiple comparison test. * $p \leq 0.05$, ** $p \leq 0.01$ and *** $p \leq 0.001$.

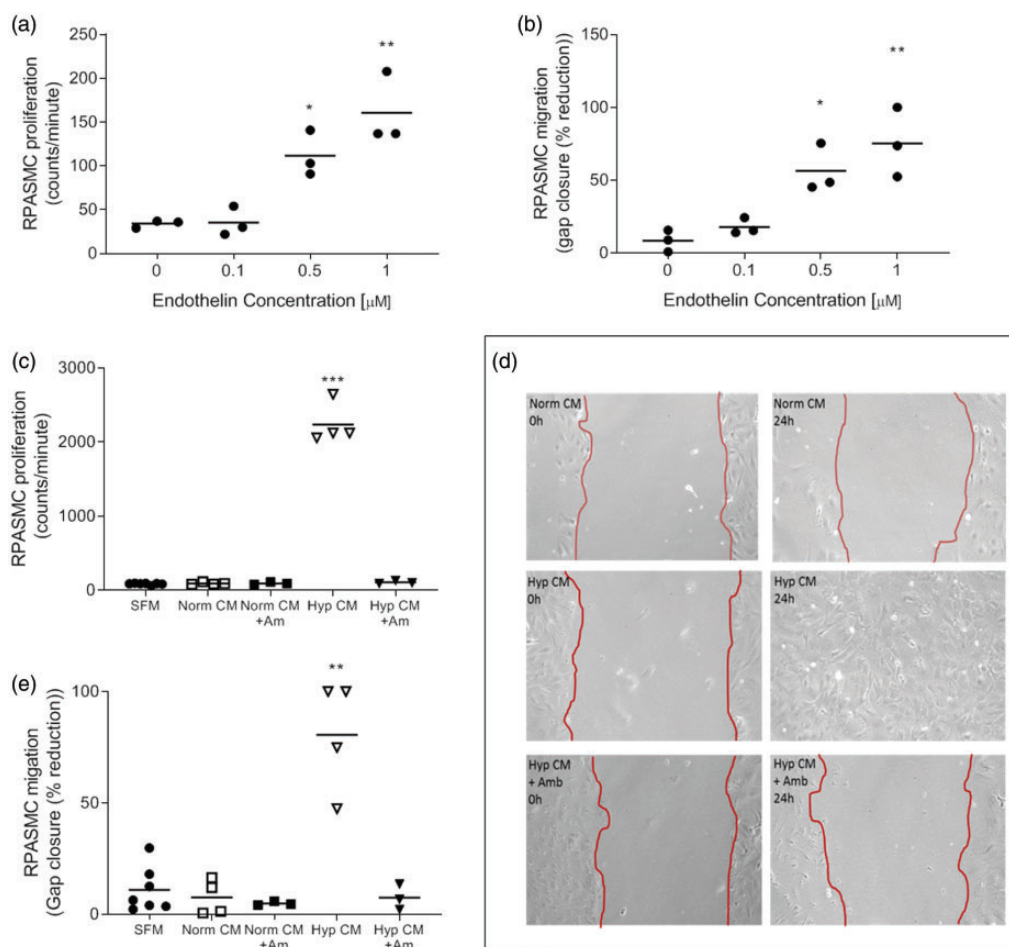


Fig. 6. Rat pulmonary artery smooth muscle cell (RPASMC) characteristics in the presence of endothelin-1 (ET-1) or endothelin receptor antagonist (ERA) Ambrisentan. Rat pulmonary artery smooth muscle cell (RPASMC) was investigated in the presence of endothelin-1 (ET-1), conditioned media from hypoxic or normoxic rat pulmonary artery fibroblast (RPAF) or the endothelin receptor antagonist (ERA) Ambrisentan. RPASMC were observed for (a) proliferative response (determined by [^3H] thymidine incorporation assay) or (b) migration (determined by scratch closure assay) following the addition of increasing concentrations of ET-1. Further to this RPASMC (c) proliferation and migration (d and e) were also investigated in the presence of conditioned media from normoxic or hypoxic RPAFs in the presence or absence of Ambrisentan. All data are $n=3-7$ biological replicates and displayed as individual with mean \pm SEM. All stats are vs SFM and analysed by one-way ANOVA and Tukey's multiple comparisons test. $*p \leq 0.01$ and $***p \leq 0.001$. SFM: serum free media.

representative model to investigate disease reversal than investigated previously²⁹ where treatment began at the end of hypoxic phase. Furthermore, there is also increasing speculation that 200 mg/kg of SU5416 may promote greater apoptotic damage to cells, particularly ECs³⁶ which may make investigation of cellular processes more complex.

Here, as expected, many of the hallmarks of PAH were observed in the SuHx animals; these include raised RVSP, RV hypertrophy, cardiac fibrosis, vascular remodelling and increased circulating levels of factors associated with disease pathogenesis. The addition of GS-444217 reversed the changes in many of these features.

It is known that the RV adapts structurally in PAH, with hypertrophy triggered by pressure overload. In contrast to previous findings,²⁹ RV hypertrophy was sustained in the present study despite a reduction observed in both RVSP

and pulmonary vascular remodelling. We believe that this demonstrates that the ASK1 inhibitor has a primary effect on the lung vasculature thus reducing RVSP. We speculate that with a reduction in RV wall stress as a consequence of reduced vascular remodelling, with time cardiac hypertrophy may also decrease. This theory is supported by a reduction in cardiomyocyte cross sectional area and a decrease in plasma BNP, features which are ordinarily hallmarks of the failing heart. BNP levels have been shown to correlate with mPAP and PVR in patients and a fall in levels after therapy is associated with improved survival.³⁷ Budas et al. state that ASK1 inhibition in their pulmonary artery banding (PAB) mouse model has an intrinsic effect on the heart, shown through a reduction in cardiac fibrosis. While not using a heart-specific model such as the PAB model, we demonstrate reduced cardiac collagen deposition in the

SuHx + GS and as these hearts have reduced pp38 MAPK, the cardiac effects may be MAPK mediated.

In our SuHx model, raised RVSP was accompanied by pulmonary artery remodelling, which the ASK1 inhibitor reversed, suggesting a direct action of ASK1 inhibition on the vascular wall. It is known that vascular remodelling observed in PAH involves changes in all three layers of the vascular wall and we have previously demonstrated the importance of the PAF in PAH^{22,38} where early activation, differentiation and subsequent migration of fibroblasts is important in vascular wall thickening.⁹ In the present study, PAF were cultured from experimental animals, we believe this to be the first time this *in vivo* to *in vitro* approach with RPAF and the SuHx model has been reported. SuHx + V cells displayed enhanced migration and proliferation under normoxic culture conditions. These cells also demonstrated enhanced pp38 MAPK abundance supporting our previous findings that proliferative and migratory response in RPAFs is mediated by MAPK signalling.^{33,39} Further supporting a role of MAPK signalling, SuHx + GS cells had reduced pp38 MAPK abundance, migration and proliferation – the first time that a phenotypic change attributed to MAPK signalling has been observed in this cell type after isolation from experimental animals treated with MAPK inhibitor.

To investigate further the role of ASK1 in PAFs, we utilised a hypoxic *in vitro* model of PH (described in detail elsewhere^{33,40}) in control PAF cells. In line with observations in cultured patient fibroblasts,⁴¹ hypoxia increased ROS and lactate production (online Supplemental Fig. 3), suggesting increased aerobic glycolysis. Hypoxia also caused a rise in the activation (phosphorylation) of many of the investigated MAPKs and HIF-1 α , the ASK1 inhibitor prevented phosphorylation of these proteins.

HIF-1 is a potent transcription factor which affects and regulates the expression of dozens of genes involved in homeostatic maintenance as oxygen concentrations change.⁴² During normoxia, the HIF-1 α subunit is polyubiquitinated and targeted for degradation by proline-hydroxylase-2 (PHD-2) and by von-Hippel-Lindau (VHL)-ubiquitin ligase complexes.⁴³ During hypoxia, the decline in oxygen levels directly decreases the activity of the PHDs, thereby preventing hydroxylation of the HIF-1 α protein.⁴⁴ The lack of hydroxylation inhibits pVHL from binding to HIF-1 α , allowing HIF-1 α to be stabilised. More recent understanding suggests that hydroxylases are not the sole regulators of HIF-1 during hypoxia but that intracellular signalling pathways are also required for activation during hypoxia. For example, it has been shown that MAPK and other kinase pathways are involved. While the upstream activators of these kinases have yet to be fully identified, ROS generated during hypoxia may be a candidate.⁴⁵

Activation of HIF-1 α is a multi-step process and emerging evidence has shown that this process involves the phosphorylation of its regulatory/inhibitory domain by p38

MAPK and other kinase signalling pathways.^{42,45,46} p38 MAPK, activated by ASK1, has been shown to phosphorylate and therefore support ischemic and LPS-dependent accumulation of HIF-1 α .⁴⁷⁻⁴⁹ Pharmacological inhibition of p38 α MAPK has also been shown to decrease hypoxic activation of HIF-1.⁵⁰ In accordance with these findings, we demonstrate that ASK1 is selectively required for the activation of p38 MAPK in the hypoxia model of PH and that p38 MAPK plays a contributory role to the hypoxia-driven activation of HIF-1 α by phosphorylation. HIF-1 α is involved in proliferation, glycolytic pathways and nitric oxide synthesis, all of which were found to be altered here and prevented by the addition of the ASK1 inhibitor (online Supplemental Fig. 3).

Hypoxia significantly increases RPAF but not RPASMC proliferation and migration when cultured alone; however, enhanced proliferation and migration were observed in RPASMCs both in co-culture and in the presence of RPAF Hyp CM. ASK1 inhibition prevented both RPAF and RPAF-mediated RPASMC-RPAF co-cultured phenotypic changes suggesting that not only are fibroblasts undergoing phenotypic changes but hypoxia sensing is being relayed to the adjacent RPASMCs. Fibroblasts have been shown to exert significant paracrine effects on other cells, producing a wide array of cytokines, growth factors and inflammatory mediators.³⁸

Whilst not the only mitogenic factor responsible for pulmonary vascular remodelling, ET-1 is one of the strongest expressed in our model. ET-1 has previously been implicated in the pathogenesis of PAH,⁵¹ it is known to be upregulated in PAH patients, and levels have been shown to correlate negatively with PVR and mPAP.⁵² Inhibition of ET-1 signalling has been shown to significantly attenuate the oxidative stress associated with PAH.⁵³ A rise in ET-1 was detected in PAF CM in our *in vitro* model of PH; interestingly when the CM of the *in vivo* to *in vitro* cells was investigated, a significant rise in ET-1 was also noted in SuHx + V compared to the other groups investigated. The synthesis and release of ET-1 from PAF has previously been linked with the regulation of other cell types in neovascularisation and angiogenesis,⁵⁴ for example ET-1 promotes vasoconstriction through a direct effect on SMC membrane-bound ET-1 receptors.⁵⁵ Confirming a role of ET-1 in this model, RPAF-stimulated PSMCs migration and proliferation could be blocked by a selective endothelin A receptor (ET_A) receptor antagonist (Ambrisentan). As ASK1 inhibition prevents this response, increased ET-1 transcription from RPAFs may be a result of the MAPK signalling pathways and HIF-1 α acting as a transcription factor.⁵⁶

ET-1 also induces fibroblast differentiation, ECM synthesis and fibrosis,^{57,58} all features noted in our study. ET-1 may have autocrine effects on RPAFs increasing its own expression via membrane-bound ET_A receptors. As ASK1 inhibition prevents the release of ET-1 into CM, this suggests that ET-1 may be driving some of the phenotypic changes in the RPAFs too.

ET-1 may also be responsible for some of the remodelling features (TIMP-1 expression and collagen deposition) in the heart observed here. PAH is characterised by increased ECM production contributing to the remodelling of the adventitia.⁵⁹ Proteolytic enzymes such as matrix metalloproteinases (MMPs) are involved in collagen degradation.⁵⁹ The activities of MMPs are counteracted by TIMPs which control the overall turnover of matrix proteins. In our study, we observed increased TIMP-1 which inhibits collagenases, stromelysin and gelatinases.⁶⁰ TIMP-1 levels were increased in both our cellular and animal models and reduced by the addition of GS-444217 suggesting that TIMP-1 is controlled by ASK1 activity.

The disparity between the *in vivo*, *in vitro* and clinical data highlights the challenges in translating pre-clinical findings into clinical success. While the pre-clinical models recapitulate many of the features of PAH pathogenesis, they do not truly replicate the complexity of the disease in the patient population; rodent and cellular studies represent a homogeneous study population, whereas it is known that PAH patients display differing genetic backgrounds, co-morbidities and are often currently on vasodilator therapies which may influence their ability to respond to novel treatments.^{61–63} It is also well recognised that inter-individual differences mean that patients can respond differently to the same PAH treatment,⁶⁴ a point highlighted by the large standard deviation observed within each group in the ARROW study.⁶⁵

In the ARROW study, patients were eligible with idiopathic or heritable PAH; drug- and toxin-induced PAH or PAH associated with connective tissue disease, HIV infection or congenital heart defects; of these idiopathic and heritable PAH represented 56% and 15% of study participants, respectively.³¹ It is likely that the causative molecular and cellular pathways contributing to disease progression differ within the patient population and it may be that any therapeutic effect noted was diluted by larger groups with limited efficacy. For example, our study highlights changes in ET-1, and while ET-1 inhibition shows some prognostic success in some patients, it is found to vary in efficacy between some subgroups of patients, for example those patients who have PAH associated with congenital heart disease.⁶⁶ Furthermore, there are ET-1 pathway polymorphisms and as such treatment responses vary in patients with PAH. A number of confounding factors such as African ethnicity, male sex and older age are associated with a raised plasma ET-1; while angiotensin-converting enzyme inhibitors, statins, β -blockers and vasodilators reduce the level of ET-1 in plasma.⁶⁷ As ASK1 inhibition displays significant success in rodent models,²⁹ it may offer a more viable treatment in more specific patient phenotypes; here, post hoc analysis of patient data may provide greater understanding.

Whilst combination therapy is an important treatment strategy for PAH, it should be highlighted that in our *in vivo* study, ASK1 was the sole treatment, in the ARROW

study, 92% of patients were on combination therapy and all were symptomatic despite therapy. It is unclear whether combined therapy could have resulted in additive, synergistic or antagonistic interactions with the ASK1 inhibitor leading to differences in efficacy, possibly explaining the lack of response in patients compared to the rodent studies.

The ARROW study duration was 24 weeks, and whilst clinical trials assessing vasoactive changes with vasodilator treatments can be observed in as little as four months of treatment, this may not have been significantly long enough to have an impact on PVR using an anti-proliferative/anti-fibrotic treatment. While positive correction in mPAP was noted in our study, the duration was perhaps not long enough to produce reversal in RVH as noted in the prevention study.²⁹

Finally, whilst the primary endpoint was not achieved in the ARROW study, it should be highlighted that a correlation of reduced PVR was seen in the higher dose groups (6 mg and 18 mg); although, this data was confounded by an increase from baseline vascular resistance in the low-dose group.⁶⁵ It should also be highlighted that there were no significant adverse events seen in the treatment group and the number of participants that had an improved WHO functional class was notably higher in the treatment groups (14–19%) when compared to the placebo group (3%).⁶⁵

Conclusion

ASK1-dependent stress-signalling pathways are known to be critical in the remodelling processes observed in PAH. Here, the selective ASK1 inhibitor (GS-444217) reduced lung vascular remodelling and subsequently RVSP in a SuHx model of PH. Furthermore, ASK1 inhibition prevented chronic hypoxia-induced proliferation and migration of RPAFs *in vitro* and prevented hypoxia-induced RPAF cytokine production and mitogenic signalling to adjacent RPASMCS, a feature which is in keeping with the multi-cellular vascular changes of PAH pathogenesis. The beneficial effects of GS-444217 appear to be as result of reduced fibroblast activation-migration, proliferation and expression of mitogenic factors such as ET-1.

The data presented here demonstrates the mechanistic role of ASK1 in remodelling associated with PAH and highlights the potential of ASK1 inhibition as a valid anti-remodelling treatment for PAH due to its positive effects on the PAF; however, it is clear that further investigation into why such compelling pre-clinical evidence has not been replicated in patient studies.

Acknowledgements

We thank Margaret Nilsen, Monika Setiawan, Andrew McNair, David Svolkinas and Tarkan Cilic Kilic for technical assistance.

Author's contributions

K.S.W. designed and performed experiments, analysed and interpreted data and wrote the manuscript. D.J.W. designed experiments, interpreted data and wrote the manuscript. H.B. and K.S. performed experiments and analysed data. G.R.B., A.C.C., M.J., J.T.L., M.R.M. and A.J.P. interpreted data. All authors were involved in critically revising the manuscript.

Conflict of interest

G.R.B. and J.T.L. are employees of Gilead Science. All other authors declare no conflicts of interest. All authors take responsibility for all aspects of the reliability and freedom from bias of the data presented and their discussed interpretation.

Funding

This study was funded as part of an industrial collaboration with Gilead Science Inc. Apoptosis signal-regulating kinase I inhibitor GS-444217 was provided by Gilead Science Inc. *In vivo* training was supported, in part, by BHF Programme Grant no. RG/16/2/32153.

Supplemental material

Supplemental material for this article is available online.

References

1. Archer SL, Weir EK and Wilkins MR. The basic science of pulmonary arterial hypertension for clinicians: new concepts and experimental therapies. *Circulation* 2010; 121: 2045–2066.
2. Aggarwal S, Gross CM, Sharma S, et al. Reactive oxygen species in pulmonary vascular remodelling. *Compr Physiol* 2013; 3: 1011–1034.
3. Nogueira-Ferreira R, Ferreira R and Henriques-Coelho T. Cellular interplay in pulmonary arterial hypertension: implications for new therapies. *Biochim Biophys Acta* 2014; 1843: 885–893.
4. Baliga RS, MacAllister RJ and Hobbs AJ. New perspectives for the treatment of pulmonary hypertension. *Br J Pharmacol* 2011; 163: 125–140.
5. Lai YC, Potoka KC, Champion HC, et al. Pulmonary arterial hypertension: the clinical syndrome. *Circ Res* 2014; 115: 115–130.
6. Jeffery TK and Wanstall JC. Pulmonary vascular remodeling: a target for therapeutic intervention in pulmonary hypertension. *Pharmacol Ther* 2001; 92: 1–20.
7. Welsh DJ and Peacock AJ. Cellular responses to hypoxia in the pulmonary circulation. *High Alt Med Biol* 2013; 14: 111–116.
8. Herrmann J, Samee S, Chade A, et al. Differential effect of experimental hypertension and hypercholesterolemia on adventitial remodeling. *Arterioscler Thromb Vasc Biol* 2005; 25: 447–453.
9. Sartore S, Chiavegato A, Faggini E, et al. Contribution of adventitial fibroblasts to neointima formation and vascular remodeling: from innocent bystander to active participant. *Circ Res* 2001; 89: 1111–1121.
10. McGrath JC, Deighan C, Briones AM, et al. New aspects of vascular remodelling: the involvement of all vascular cell types. *Exp Physiol* 2005; 90: 469–475.
11. DeMarco VG, Whaley-Connell AT, Sowers JR, et al. Contribution of oxidative stress to pulmonary arterial hypertension. *World J Cardiol* 2010; 2: 316–324.
12. Bowers R, Cool C, Murphy RC, et al. Oxidative stress in severe pulmonary hypertension. *Am J Respir Crit Care Med* 2004; 169: 764–769.
13. Crosswhite P and Sun Z. Nitric oxide, oxidative stress and inflammation in pulmonary arterial hypertension. *J Hypertens* 2010; 28: 201–212.
14. Touyz RM. Reactive oxygen species, vascular oxidative stress, and redox signaling in hypertension: what is the clinical significance? *Hypertension* 2004; 44: 248–252.
15. Freund-Michel V, Guibert C, Dubois M, et al. Reactive oxygen species as therapeutic targets in pulmonary hypertension. *Ther Adv Respir Dis* 2013; 7: 175–200.
16. Irukayama-Tomobe Y, Sakai S and Miyauchi T. Chronic treatment with probucol effectively inhibits progression of pulmonary hypertension in rats. *Life Sci* 2000; 67: 2017–2023.
17. Uzun O, Balbay O, Comunoglu NU, et al. Hypobaric-hypoxia-induced pulmonary damage in rats ameliorated by antioxidant erdosteine. *Acta Histochem* 2006; 108: 59–68.
18. Nozik-Grayck E and Stenmark KR. Role of reactive oxygen species in chronic hypoxia-induced pulmonary hypertension and vascular remodeling. In: Roach RC, Wagner PD and Hackett PH (eds) *Hypoxia and the circulation advances in experimental medicine and biology*. 618. 2008/02/14 ed. Boston, MA: Springer, 2007, pp.101–112.
19. McCubrey JA, Lahair MM and Franklin RA. Reactive oxygen species-induced activation of the MAP kinase signaling pathways. *Antioxid Redox Signal* 2006; 8: 1775–1789.
20. Son Y, Kim S, Chung HT, et al. Reactive oxygen species in the activation of MAP kinases. *Methods Enzymol* 2013; 528: 27–48.
21. Soon E, Holmes AM, Treacy CM, et al. Elevated levels of inflammatory cytokines predict survival in idiopathic and familial pulmonary arterial hypertension. *Circulation* 2010; 122: 920–927.
22. Church AC, Martin DH, Wadsworth R, et al. The reversal of pulmonary vascular remodeling through inhibition of p38 MAPK- α : a potential novel anti-inflammatory strategy in pulmonary hypertension. *Am J Physiol Lung Cell Mol Physiol* 2015; 309: L333–L347.
23. Tormos AM, Talens-Visconti R, Nebreda AR, et al. p38 MAPK: a dual role in hepatocyte proliferation through reactive oxygen species. *Free Radic Res* 2013; 47: 905–916.
24. Torres M and Forman HJ. Redox signaling and the MAP kinase pathways. *Biofactors* 2003; 17: 287–296.
25. Dabrowski A, Boguslowicz C, Dabrowska M, et al. Reactive oxygen species activate mitogen-activated protein kinases in pancreatic acinar cells. *Pancreas* 2000; 21: 376–384.
26. Nagai H, Noguchi T, Takeda K, et al. Pathophysiological roles of ASK1-MAP kinase signaling pathways. *J Biochem Mol Biol* 2007; 40: 1–6.
27. Soga M, Matsuzawa A and Ichijo H. Oxidative stress-induced diseases via the ASK1 signaling pathway. *Int J Biochem Cell Biol* 2012; 2012: 439587.
28. Hayakawa R, Hayakawa T, Takeda K, et al. Therapeutic targets in the ASK1-dependent stress signaling pathways. *Proc Jpn Acad Ser B Phys Biol Sci* 2012; 88: 434–453.
29. Budas GR, Boehm M, Kojonazarov B, et al. ASK1 inhibition halts disease progression in preclinical models of pulmonary

- arterial hypertension. *Am J Respir Crit Care Med* 2018; 197: 373–385.
30. Liles J, Budas G, Liang F, et al. ASK1 promotes maladaptive remodeling in a rodent model of pulmonary hypertension. *Eur Respir J* 2014; 44: 2298.
 31. Rosenkranz S, Feldman J, McLaughlin V, et al. The ARROW study: a phase 2, prospective, randomized, double-blind, placebo-controlled study of selonsertib in subjects with pulmonary arterial hypertension. *Eur Respir J* 2017; 50.
 32. Freshney RI. *Culture of animal cells: a manual of basic technique and specialized applications*. 6th ed – Student Companion Site. Hoboken, NJ: John Wiley & Sons, 2010.
 33. Welsh DJ, Peacock AJ, MacLean M, et al. Chronic hypoxia induces constitutive p38 mitogen-activated protein kinase activity that correlates with enhanced cellular proliferation in fibroblasts from rat pulmonary but not systemic arteries. *Am J Respir Crit Care Med* 2001; 164: 282–289.
 34. Taraseviciene-Stewart L, Kasahara Y, Alger L, et al. Inhibition of the VEGF receptor 2 combined with chronic hypoxia causes cell death-dependent pulmonary endothelial cell proliferation and severe pulmonary hypertension. *FASEB J* 2001; 15: 427–438.
 35. De Raaf MA, Schalij I, Gomez-Arroyo J, et al. SuHx rat model: partly reversible pulmonary hypertension and progressive intima obstruction. *Eur Respir J* 2014; 44: 160–168.
 36. Rafikova O, Rafikov R, Meadows ML, et al. The sexual dimorphism associated with pulmonary hypertension corresponds to a fibrotic phenotype. *Pulm Circ* 2015; 5: 184–197.
 37. Casserly B and Klinger JR. Brain natriuretic peptide in pulmonary arterial hypertension: biomarker and potential therapeutic agent. *Drug Des Devel Ther* 2009; 3: 269–287.
 38. Pak O, Aldashev A, Welsh D, et al. The effects of hypoxia on the cells of the pulmonary vasculature. *Eur Respir J* 2007; 30: 364–372.
 39. Mortimer HJ, Peacock AJ, Kirk A, et al. p38 MAP kinase: essential role in hypoxia-mediated human pulmonary artery fibroblast proliferation. *Pulm Pharmacol Ther* 2007; 20: 718–725.
 40. Scott PH, Paul A, Belham CM, et al. Hypoxic stimulation of the stress-activated protein kinases in pulmonary artery fibroblasts. *Am J Respir Crit Care Med* 1998; 158: 958–962.
 41. Plecita-Hlavata L, Tauber J, Li M, et al. Constitutive reprogramming of fibroblast mitochondrial metabolism in pulmonary hypertension. *Am J Respir Cell Mol* 2016; 55: 47–57.
 42. Yoon D, Pastore YD, Divoky V, et al. Hypoxia-inducible factor-1 deficiency results in dysregulated erythropoiesis signaling and iron homeostasis in mouse development. *J Biol Chem* 2006; 281: 25703–25711.
 43. Ziello JE, Jovin IS and Huang Y. Hypoxia-inducible factor (HIF)-1 regulatory pathway and its potential for therapeutic intervention in malignancy and ischemia. *Yale J Biol Med* 2007; 80: 51–60.
 44. Hirsila M, Koivunen P, Gunzler V, et al. Characterization of the human prolyl 4-hydroxylases that modify the hypoxia-inducible factor. *J Biol Chem* 2003; 278: 30772–30780.
 45. Sodhi CP, Phadke SA, Batlle D, et al. Hypoxia stimulates osteopontin expression and proliferation of cultured vascular smooth muscle cells: potentiation by high glucose. *Diabetes* 2001; 50: 1482–1490.
 46. Minet E, Michel G, Mottet D, et al. Transduction pathways involved in Hypoxia-Inducible Factor-1 phosphorylation and activation. *Free Radic Biol Med* 2001; 31: 847–855.
 47. Sumbayev VV. LPS-induced Toll-like receptor 4 signalling triggers cross-talk of apoptosis signal-regulating kinase 1 (ASK1) and HIF-1 α protein. *FEBS Lett* 2008; 582: 319–326.
 48. Kwon SJ, Song JJ and Lee YJ. Signal pathway of hypoxia-inducible factor-1 alpha phosphorylation and its interaction with von Hippel–Lindau tumor suppressor protein during ischemia in MiaPaCa-2 pancreatic cancer cells. *Clin Cancer Res* 2005; 11: 7606–7616.
 49. Pchejetski D, Nunes J, Coughlan K, et al. The involvement of sphingosine kinase 1 in LPS-induced Toll-like receptor 4-mediated accumulation of HIF-1 α protein, activation of ASK1 and production of the pro-inflammatory cytokine IL-6. *Immunol Cell Biol* 2011; 89: 268–274.
 50. Hirota K and Semenza GL. Rac1 activity is required for the activation of hypoxia-inducible factor 1. *J Biol Chem* 2001; 276: 21166–21172.
 51. Shao D, Park JE and Wort SJ. The role of endothelin-1 in the pathogenesis of pulmonary arterial hypertension. *Pharmacol Res* 2011; 63: 504–511.
 52. Galie N, Manes A and Branzi A. The endothelin system in pulmonary arterial hypertension. *Cardiovasc Res* 2004; 61: 227–237.
 53. Rafikova O, Rafikov R, Kumar S, et al. Bosentan inhibits oxidative and nitrosative stress and rescues occlusive pulmonary hypertension. *Free Radic Biol Med* 2013; 56: 28–43.
 54. Davie NJ, Gerasimovskaya EV, Hofmeister SE, et al. Pulmonary artery adventitial fibroblasts cooperate with vasa vasorum endothelial cells to regulate vasa vasorum neovascularization: a process mediated by hypoxia and endothelin-1. *Am J Pathol* 2006; 168: 1793–1807.
 55. Kim FY, Barnes EA, Ying L, et al. Pulmonary artery smooth muscle cell endothelin-1 expression modulates the pulmonary vascular response to chronic hypoxia. *Am J Physiol Lung Cell Mol Physiol* 2015; 308: L368–L377.
 56. Yamashita K, Discher DJ, Hu J, et al. Molecular regulation of the endothelin-1 gene by hypoxia. Contributions of hypoxia-inducible factor-1, activator protein-1, GATA-2, and p300/CBP. *J Biol Chem* 2001; 276: 12645–12653.
 57. Shi-Wen X, Chen Y, Denton CP, et al. Endothelin-1 promotes myofibroblast induction through the ETA receptor via a rac/phosphoinositide 3-kinase/Akt-dependent pathway and is essential for the enhanced contractile phenotype of fibrotic fibroblasts. *Mol Biol Cell* 2004; 15: 2707–2719.
 58. Xu SW, Howat SL, Renzoni EA, et al. Endothelin-1 induces expression of matrix-associated genes in lung fibroblasts through MEK/ERK. *J Biol Chem* 2004; 279: 23098–23103.
 59. Budhiraja R, Tuder RM and Hassoun PM. Endothelial dysfunction in pulmonary hypertension. *Circulation* 2004; 109: 159–165.
 60. Vieillard-Baron A, Frisdal E, Eddahibi S, et al. Inhibition of matrix metalloproteinases by lung TIMP-1 gene transfer or doxycycline aggravates pulmonary hypertension in rats. *Circ Res* 2000; 87: 418–425.
 61. Badlam JB and Bull TM. Steps forward in the treatment of pulmonary arterial hypertension: latest developments and clinical opportunities. *Ther Adv Chronic Dis* 2017; 8: 47–64.

62. Humbert M, Lau EM, Montani D, et al. Advances in therapeutic interventions for patients with pulmonary arterial hypertension. *Circulation* 2014; 130: 2189–2208.
63. Hill NS, Cawley MJ and Heggen-Peay CL. New therapeutic paradigms and guidelines in the management of pulmonary arterial hypertension. *J Manag Care Spec Pharm* 2016; 22: S3–S21.
64. Halliday SJ and Hemnes AR. Identifying “super responders” in pulmonary arterial hypertension. *Pulm Circ* 2017; 7: 300–311.
65. Ogier JM, Nayagam BA and Lockhart PJ. ASK1 inhibition: a therapeutic strategy with multi-system benefits. *J Mol Med (Berl)* 2020; 98: 335–348.
66. Barst RJ. Sitaxsentan: a selective endothelin – a receptor antagonist, for the treatment of pulmonary arterial hypertension. *Expert Opin Pharmacother* 2007; 8: 95–109.
67. Shah R. Endothelins in health and disease. *Eur J Intern Med* 2007; 18: 272–282.